On the Thermomechanical Response of HTPB-Based Composite Beams Under Near-Resonant Excitation

Daniel C. Woods
School of Mechanical Engineering,
Birck Nanotechnology Center and
Ray W. Herrick Laboratories,
Purdue University,
West Lafayette, IN 47907

Jacob K. Miller
School of Mechanical Engineering,
Birck Nanotechnology Center and
Ray W. Herrick Laboratories,
Purdue University,
West Lafayette, IN 47907

Jeffrey F. Rhoads[1]
School of Mechanical Engineering,
Birck Nanotechnology Center and
Ray W. Herrick Laboratories,
Purdue University,
West Lafayette, IN 47907
e-mail: jfrhoads@purdue.edu

Currently, there is a pressing need to detect and identify explosive materials in both military and civilian settings. While these energetic materials vary widely in both form and composition, many traditional explosives consist of a polymeric binder material with embedded energetic crystals. Interestingly, many polymers exhibit considerable self-heating when subjected to harmonic loading, and the vapor pressures of many explosives exhibit a strong dependence on temperature. In light of these facts, thermomechanics represent an intriguing pathway for the stand-off detection of explosives, as the thermal signatures attributable to motion-induced heating may allow target energetic materials to be distinguished from their more innocuous counterparts. In the present work, the thermomechanical response of a sample from this class of materials is studied in depth. Despite the nature of the material as a polymer-based particulate composite, classical Euler–Bernoulli beam theory, along with the complex modulus representation for linear viscoelastic materials, was observed to yield predictions of the thermal and mechanical responses in agreement with experimental investigations. The results of the experiments conducted using a hydroxyl-terminated polybutadiene (HTPB) beam with embedded ammonium chloride (NH_4Cl) crystals are presented. Multiple excitation levels are employed and the results are subsequently compared to the work's analytical findings. [DOI: 10.1115/1.4029996]

1 Introduction

To address matters of security in military and civilian settings, there is, at present, a significant need for new technologies capable of detecting explosive materials. Though there is a wide variety of detection systems currently in use, many exploit the volatility of energetic materials and detect the saturated vapors that exist near the materials' surfaces [1,2]. Unfortunately, vapor pressures drop significantly if the explosive materials are sealed or packed in a bag, or both, which is often the case [3]. These pressures also drop considerably in certain environments, such as with strong winds and at lower temperatures. As such, trace vapor detection of improvised explosive devices remains a substantial technical challenge.

Given the strong dependence of vapor pressure on temperature [4], explosive detection capabilities may be significantly enhanced by heating the target material. Though energetic materials vary widely in form and composition, many traditional explosives consist of a polymeric binder material with embedded energetic crystals. Polymers exhibit considerable self-heating when subjected to harmonic loading, owing to distinctly out-of-phase stress and strain oscillations [5]. In addition, low-frequency mechanical and acoustic excitations can be transmitted over relatively large distances, allowing for stand-off excitation. Taken collectively, these seemingly disparate statements suggest that thermomechanics may provide an intriguing pathway for explosives detection, as the self-heating response of explosive materials to low-frequency excitation may be exploited to increase vapor pressure from a stand-off distance, and thus increase the relative utility of vapor-based detection systems. However, for this particular class of materials, the elicited thermal response under mechanical loading has not been studied in depth, to the best of the authors' knowledge.

Heat generation in response to mechanical or acoustic excitation is well-documented for pure materials and composites. Thermomechanical coupling is described by the thermodynamic theory of solids, which is inclusive of both viscoelastic and thermoelastic effects [6]. Thermal responses are elicited along modal structures due to material damping [7] and are particularly exacerbated near stress concentrations, which is commonly exploited in the field of vibrothermography [8,9] to identify structural defects. The related self-heating effect has been documented in polymeric materials and polymer-based composites [10,11], including particulate composites, for which the particle/binder ratio is known to have a strong impact on material properties [12,13]. For explosive materials, the works of Loginov et al. [14,15] provide insight into the nature of the heating of explosives subjected to mechanical excitation.

The aim of this work is to characterize the thermomechanical response of a polymeric particulate composite material subjected to mechanical excitation, with an eye toward explosives detection. Specifically, a viscoelastic model is applied to predict the thermomechanical behavior of an HTPB beam with embedded ammonium chloride (NH_4Cl) crystals subjected to harmonic mechanical loading. The sample composition, also used in previous work [13], is a mock mechanical material intended to resemble common plastic-bonded energetic materials. Despite the nature of the polymeric composite considered here, classical Euler–Bernoulli beam theory, along with a homogenized material model for linear viscoelastic materials, was observed to yield predictions of the thermal and mechanical responses in agreement with experimental investigations. With the goal of maximizing self-heating for the application of trace vapor detection, near-resonant excitations are considered. The thermal and mechanical responses of the sample are recorded using infrared thermography and scanning laser Doppler vibrometry. Multiple excitation levels are employed and the results are subsequently compared to the work's analytical findings.

2 Modeling of a Thin Polymer-Based Beam Subjected to Harmonic Excitation

Thermomechanical coupling in polymers is due to both reversible thermoelastic effects and internal energy dissipation. Experiments show that under intensive loading, the dominant mechanism in polymers is internal dissipation [16], generally described by a viscoelastic model. During harmonic loading, the energy losses caused by out-of-phase oscillations between stress and strain generate heat [11]. Due to the poor thermal conductivity

[1]Corresponding author.

Contributed by the Technical Committee on Vibration and Sound of ASME for publication in the JOURNAL OF VIBRATION AND ACOUSTICS. Manuscript received February 12, 2015; final manuscript received February 22, 2015; published online April 27, 2015. Editor: I. Y. (Steve) Shen.

of most polymers, this leads to considerable self-heating. The temperature of the polymer rises until a thermal steady-state is reached, at which point the heat dispelled to the environment balances that generated from dissipation. Thermal runaway is also possible [17].

2.1 Equation of Motion. The polymeric particulate composite material of interest here is modeled as a homogenized linear viscoelastic material. The utilized x-axis is defined along the beam axis at the centroid of the rectangular cross section. The beam is subjected to harmonic excitation in the transverse, y, direction, and the z-axis lies along the width dimension. The beam has length L, thickness h, and width b.

In modeling the mechanical response, the standard assumptions of Euler–Bernoulli beam theory [18] are used and the equation for transverse motion is thus given by

$$D^*(\omega,\theta)\frac{\partial^4 u}{\partial x^4}+\rho h\frac{\partial^2 u}{\partial t^2}=f^* \tag{1}$$

where, using complex quantities where appropriate, u is the transverse displacement of the neutral surface, t is the time variable, ω is the circular forcing frequency, θ is the temperature of the material as measured from ambient, ρ is the mass density, f^* is the forcing function per unit area, and D^* is the flexural rigidity, which is given by

$$D^*(\omega,\theta)=\frac{E^*(\omega,\theta)h^3}{12[1-\nu^2(\omega,\theta)]} \tag{2}$$

where E^* is the complex modulus [19,20], and ν is Poisson's ratio. For beams with a considerable aspect ratio (b/h), the effective stiffness is increased due to the two-dimensional effect in the xz-plane, as in platelike bending [18,21]. Accordingly, the flexural rigidity for a thin plate is used, which accounts for the effect of Poisson's ratio on the flexural stiffness.

Considered here is the case for which the ends of the beam, $x=0$ and $x=L$, are subjected to a harmonic acceleration, $Ae^{i\omega t}$. The suspended beam is then under inertial excitation with the complex forcing function f^* set to zero and the transverse displacement of the form $u(x,t)=(A/\omega^2)e^{i\omega t}+\tilde{u}(x,t)$, where $\tilde{u}$ is the relative deflection resulting from the base excitation $(A/\omega^2)e^{i\omega t}$. The equation for transverse motion becomes

$$D^*(\omega,\theta)\frac{\partial^4 \tilde{u}}{\partial x^4}+\rho h\frac{\partial^2 \tilde{u}}{\partial t^2}=\rho hAe^{i\omega t} \tag{3}$$

The beam is clamped on both ends and, using the normal mode approach [18], the steady-state displacement can be computed as

$$\tilde{u}(x,t)=\sum_{n=1}^{\infty}U_n(x)\frac{\rho hA\int_0^L U_n(x)\mathrm{d}x}{D^*(\omega,\theta)\beta_n^4-\rho h\omega^2}e^{i\omega t} \tag{4}$$

where the U_n are the mode shapes for a clamped–clamped beam, normalized such that $\int_0^L U_n^2\mathrm{d}x=1$, and the β_n are the nth positive roots of the corresponding characteristic equation [18].

2.2 Heat Transfer Equation. Given that the polymer composite is modeled as a homogenized linear viscoelastic material, thermal isotropy is assumed as well. In addition, the material's thermal properties are modeled as constant and the effects of thermal expansion are neglected for the small temperature fluctuations considered. Using the Fourier law of conduction and considering heat diffusion in all three dimensions, the heat transfer equation is [22]

$$\frac{\partial^2\theta}{\partial x^2}+\frac{\partial^2\theta}{\partial y^2}+\frac{\partial^2\theta}{\partial z^2}+\frac{1}{k}r=\frac{1}{\alpha}\frac{\partial\theta}{\partial t} \tag{5}$$

where k is the thermal conductivity, α is the thermal diffusivity, and r is the volumetric energy generation. The volumetric energy generation is computed analytically here and used in conjunction with numerical methods to recover the predicted temperature distributions.

The mechanical energy dissipated in the beam per cycle of harmonic loading can be approximated as the area under the hysteresis loop of the stress–strain plot in the mechanical steady-state [19,20]. Assuming that the temperature varies on a much slower order than the mechanical loading, the volumetric energy generation can be time-averaged over one mechanical loading cycle [17]. For a thin beam, the volumetric energy generation can also be spatially averaged over the thickness [7]. If the energy is dissipated solely as heat, then the resulting volumetric energy generation is

$$r(x)=\frac{E'\eta\omega h^2}{24(1-\nu^2)}\kappa_0^2(x) \tag{6}$$

where E' is the storage modulus, η is the material loss factor, and κ_0 is the maximum value (over one cycle) of the curvature, as given by Euler–Bernoulli theory.

If a thermal steady-state is reached, the heat lost to the environment balances that generated from dissipation, though thermal runaway can occur, for example, in materials with sufficiently poor thermal conductivity [17]. In this work, the transient temperature behavior is investigated in a three-dimensional (3D) numerical simulation using the heat source given in Eq. (6).

3 Experimental Study of a Particulate Composite Beam

Experiments were conducted using an HTPB beam with embedded NH_4Cl crystals. These ammonium chloride crystals were selected to approximate the particle sizes of ammonium perchlorate (AP), and, as such, the sample serves as a mechanical mock material for common plastic-bonded energetic composites. The thermal and mechanical responses of the sample were recorded using infrared thermography and scanning laser Doppler vibrometry, as subsequently described.

3.1 Sample Preparation. To create the experimental sample, powder-form HTPB was heated to 60 °C and allowed to harden using an isocyanate agent. For mixing with the NH_4Cl crystals, a wetting agent, Tepanol, was applied and a Resodyn acoustic mixer was used to ensure homogeneity. The mixture, targeted to be 75% NH_4Cl by volume, was poured into a purpose-built plate mold and cured overnight, and then cut into a beam measuring $25.6\times2.5\times1.4$ cm. The density of the beam was computed from direct length and mass measurements as 1028.2 kg/m^3. This density is significantly lower than what would be predicted by a linear mix of the densities of pure HTPB and crystalline NH_4Cl, a discrepancy likely attributable to voids in the mixture.

3.2 Experimental Setup. A TIRA 59335/LS AIT-440 electrodynamic shaker was used to provide mechanical excitation to the beam, allowing for band-limited white noise or single-frequency harmonic inertial excitation. A VibeLab VL-144 vibration control system was employed to control the system through direct monitoring of an accelerometer mounted on the shaker head. The beam was attached to the shaker using a custom fixture, which was machined to simulate clamped boundaries on both short ends of the beam. The final mounting yielded a 22.9 cm (9 in.) unsupported length. The frequency responses and operational deflection shapes of the beam were recorded using a Polytec PSV-400 scanning laser Doppler vibrometer. The test sample and experimental apparatus are shown in Fig. 1.

For the purposes of mechanical analysis, broadband (10–1000 Hz) white noise excitation was applied at three forcing

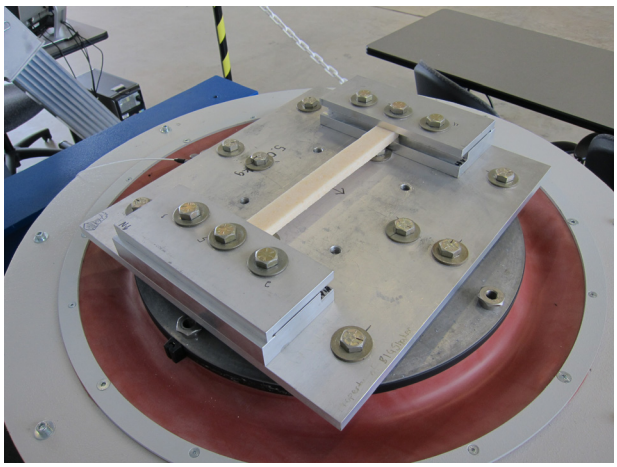

Fig. 1 The experimental sample, an HTPB beam with embedded NH_4Cl crystals, mounted on a TIRA 59335/LS AIT-440 electrodynamic shaker

levels (1, 1.86, and 2.44 g root mean square (RMS)). The system response was estimated using the classical H1 estimator, which compares the measured cross-spectral density of the accelerometer and vibrometer readings to the measured power spectral density of the accelerometer. The H1 frequency response estimators were calculated at two distinct points, the geometric center of the top face of the beam and an offset point on the top face, for all three forcing levels. The offset point was located one quarter of the distance along the beam, on the centerline.

The transient and steady-state thermal responses of the top face were recorded using a FLIR A325 thermal camera, which has a temperature sensitivity of 0.07 °C at 30 °C and an accuracy of ±2 °C or ±2%. The infrared data were calibrated to the emissivity of the beam using a thermocouple at ambient conditions. For thermal testing, the beam was excited near first resonance for 60 mins and was seen to approach thermal steady-state within this time. Though no attempt was made to control the ambient temperature or flow conditions, neither was observed to change significantly for the duration of the experiment.

4 Numerical Simulation

To solve the heat transfer equation highlighted above, numerical methods were employed. A 3D finite element simulation, implemented in COMSOL, was utilized to compute the mechanical response of the beam and numerically solve the three-dimensional problem of heat diffusion using the heat source given in Eq. (6). The density value was specified as 1028.2 kg/m^3, as obtained from direct measurement. The Poisson's ratio was estimated as 0.39, based on perceived similarities to more common materials. The storage modulus was estimated from the resonant response of a cylindrical sample of the same HTPB composite as 83.57 MPa [23]. The material loss factor was estimated as 0.35 by using the half-power bandwidth method on data taken from experimental frequency responses [24].

The thermal conductivity and thermal diffusivity were measured using the transient plane source technique [25] as 0.52 W/(m K) and 3.13×10^{-7}m^2/s, respectively. In the finite element simulation, the heat source was applied to a 259-node 3D mesh with insulated boundary conditions on the beam's ends and convective conditions elsewhere, using a convection coefficient of 5 W/(m^2 K) in an attempt to match the transient behavior observed experimentally. This convection coefficient is comparable with values recovered in experimental investigations [26–28] and is within the range for free convection estimates given in Ref. [22]. The simulation was used to generate the transient behavior over 60 mins, as well as top-down thermal profiles, which allow for direct comparison to the experimentally obtained thermal images.

5 Results and Discussion

5.1 Mechanical Response. The H1 frequency response estimators for the beam in response to the three levels of band-limited white noise excitation are presented as Fig. 2. Data at both the center and offset points on the top face are presented. The beam exhibits multiple clear resonant peaks, which decrease slightly in relative amplitude and frequency as the forcing level increases.

The beam was also excited with harmonic forcing at the first resonant frequency, which was estimated from the H1 frequency response estimators for each of the respective forcing levels. The system model approximates the mechanical behavior of the particulate composite to an acceptable degree, with errors on the order of 5% in the measured response amplitude at the center of the beam compared to the theoretical prediction. Due to the imperfect nature of the clamping fixture, which results in some rotation at the ends, there are notable deviations in the predicted values near the fixture, resulting in higher local predicted stresses as compared to the stresses encountered in the experiment.

5.2 Thermal Response. With the beam excited with 1 g, 2 g, and 3 g harmonic forcing near the first natural frequency, the transient thermal response of the top surface was recorded. The recorded maximum and mean transient surface temperatures are presented as Fig. 3. Due to the intrinsic noise in infrared temperature measurement, the data points presented represent the average of five temporally adjacent thermal measurements. For each of the forcing levels, the temperatures asymptotically approach steady-state values in the 60 mins of recording time. In general, greater forcing levels lead to greater heating, and the maximum recorded surface temperatures increase with forcing level. The highest mean surface temperatures are for 3 g forcing, though the recorded mean temperatures for 1 g and 2 g forcing are comparable. In addition, the largest separation between the maximum and mean temperatures was recorded for the 3 g forcing.

The surface temperature distributions recorded after 60 mins are presented in Fig. 4. Maximal heating was recorded near the center of the surface for all forcing levels. The axial variation of the temperature is observed to coincide with the stress and strain fields expected with a linear viscoelastic material. The volumetric heat generation is proportional to the square of the strain magnitude, as is given in Eq. (6) for the particular case of an Euler–Bernoulli beam. This effect is especially prominent with the 2 g and 3 g forcing levels, where higher local temperatures are observed in areas of high local stress near the ends of the beam.

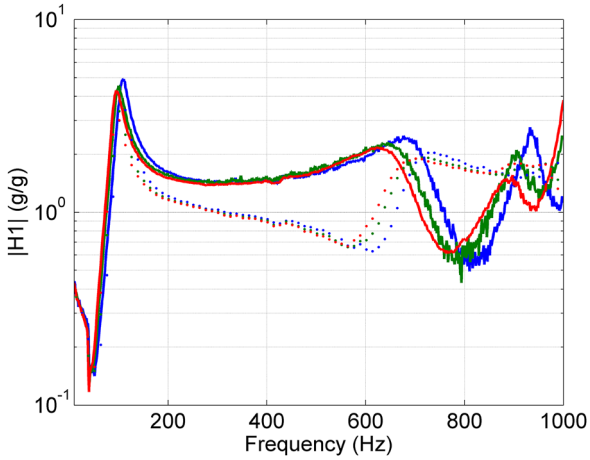

Fig. 2 The experimental H1 mechanical frequency response estimators for three levels of excitation. The blue, green, and red curves represent responses at 1, 1.86, and 2.44 g RMS, respectively (see color version online). Solid lines correspond to data from the center point and dashed lines correspond to data from the offset point.

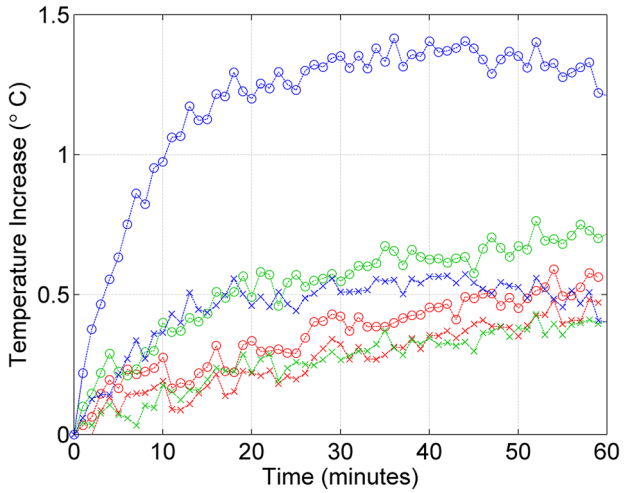

Fig. 3 The experimental maximum and mean transient surface temperatures obtained with harmonic forcing near the first natural frequency. The red, green, and blue data points represent responses to forcing at 1 g, 2 g, and 3 g, respectively (see color version online). Circles correspond to maximum surface temperatures and "x" correspond to mean surface temperatures.

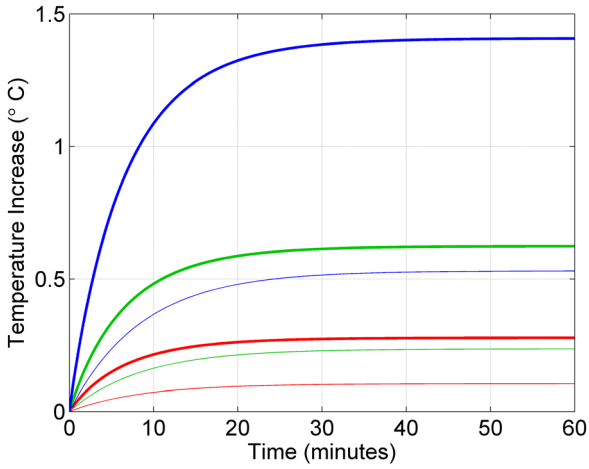

Fig. 5 The maximum and mean transient surface temperatures obtained in the 3D numerical simulation with harmonic forcing near the first natural frequency. The red, green, and blue curves represent responses to forcing at 1 g, 2 g, and 3 g, respectively (see color version online). Bold lines correspond to maximum surface temperatures and thin lines correspond to mean surface temperatures.

Variations in temperature through the width of the beam are attributable to the convective boundaries on each surface. Specifically, heat is dispelled to the environment at the surfaces and greater temperatures are generated at the center, farthest away from those surfaces. The effects of the stress field and convective boundaries interact in the surface temperature distributions recorded. The lesser prominence of structure for the 1 g forcing level is due to the comparatively lower temperature deviations recovered.

The numerical simulation results for the maximum and mean transient surface temperatures at all three forcing levels are presented in Fig. 5. The steady-state surface temperature distribution recovered from the simulation for 3 g harmonic excitation is presented in Fig. 6. The temperature magnitudes obtained from the 3D simulation show reasonable agreement with the recorded values, and the steady-state surface temperature distribution shows a character consistent with the distribution recorded at 3 g forcing. A local region of higher temperatures is generated near the center and the effect of the convective boundaries is apparent at the edges. The simulation also captures the higher relative temperatures at the ends of the beam, but the observed effect is magnified

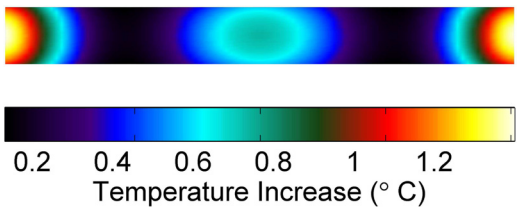

Fig. 6 The steady-state surface temperature distribution obtained in the 3D numerical simulation in response to 3 g harmonic forcing near the first natural frequency

as compared to experiments. This is attributable to the fact that insulated boundaries at the ends were assumed in the model, whereas in the experiment there is additional material at the ends, along with contact with the fixture, which yields a nonzero heat flux. Also, as previously noted, the imperfect nature of the clamping fixture leads to higher predicted stresses near the ends of the beam when they are modeled as clamped boundaries, which also

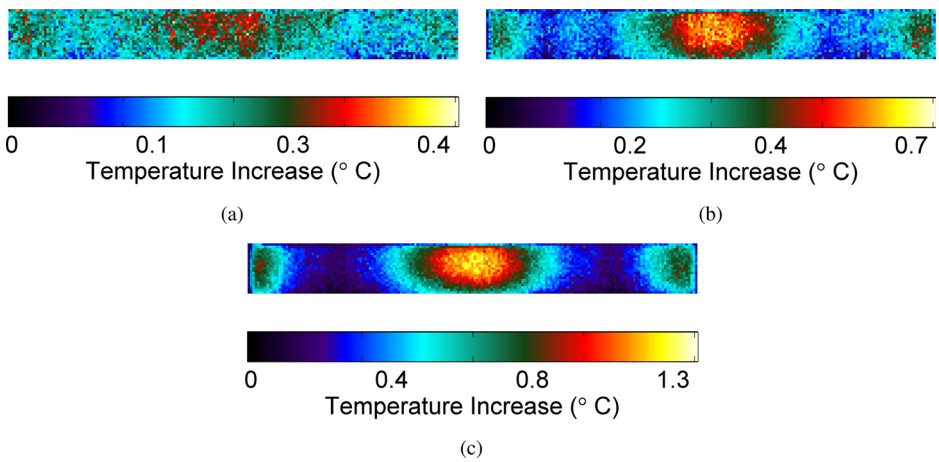

Fig. 4 The experimental surface temperature distribution recorded after 60 mins in response to harmonic forcing at: (*a*) 1 g; (*b*) 2 g; and (*c*) 3 g. Forcing was near the first natural frequency for each case.

contributes to the higher temperatures at the ends of the beam in the simulation.

6 Conclusions

A thermomechanical model of a polymeric particulate composite beam has been presented, wherein the composite is modeled as a homogenized linear viscoelastic material. The composition under consideration, which consists of an HTPB binder with embedded NH_4Cl crystals, is intended to resemble common plastic-bonded energetic materials. Despite the material composition as a particulate composite, classical Euler–Bernoulli beam theory, along with the complex modulus model for viscoelastic materials, yielded predictions of the thermal and mechanical responses consistent with experimental measurements. The acquired results revealed a strong dependence of the thermal response on the stress and strain fields produced within the beam. In addition to modal structure, convection at the surfaces was shown to impact the thermal response, and temperature excursions were noted near the center of the beam geometry.

Since explosive vapor pressures exhibit a strong dependence on temperature, the capabilities of vapor-based detection systems may be enhanced significantly by heating. Heat generation in response to harmonic excitation increases, as noted, with strain magnitude and, for a given strain level, with forcing frequency. The strain magnitude may be increased with greater forcing levels or selective boundary conditions, though obviously there is limited control over boundary conditions in many explosives detection systems. Heat generation is also intensified as the phase difference between stress and strain oscillations, quantified by the material loss factor, is increased. The phase difference depends on the forcing level and frequency [19], and thus may be used to enhance heating. Though heating also depends on other moduli, there is little control over material properties and sample geometry in explosives detection applications.

It should also be noted that the authors have explored various nonlinear structural mechanics mechanisms as a means of eliciting greater heating. These investigations have leveraged the fact that at large strain levels, geometric nonlinearities are significant. Unfortunately, the forcing levels necessary to exploit such behaviors for appreciably enhanced heating, at least within the context of the polymeric particulate composite considered here, are too large to achieve in practice, where excitations up to approximately 10 g are considered attainable.

In addition to the structural heating considered in this work, microscale heating of energetic materials through laser or ultrasonic excitation [29–31] may also constitute a viable pathway to improved trace vapor detection capabilities. Targeting local *hot spots* in the composite structure can result in greater thermal responses, but doing so generally requires proximal access to the material's surface. In contrast, low-frequency acoustic excitations can be transmitted over large distances, and thus may be used for stand-off heating, though the proportionality of heat generation to forcing frequency and the dependence of the stress–strain phase lag would have to be considered in the design of an effective stand-off detection system.

Acknowledgment

This research was supported by the U.S. Office of Naval Research as a Multidisciplinary University Research Initiative on Sound and Electromagnetic Interacting Waves under ONR Grant No. N00014-10-1-0958. The authors would like to acknowledge Christopher Watson and Professor Douglas Adams for their work in sample preparation, as well as Jelena Paripovic and Professor Patricia Davies for mechanical property measurements, and Jesus Mares, Professor Lori Groven, and Professor Steven Son for thermal property measurements. A preliminary version of this work appeared in the proceedings of the ASME 2014 International Design Engineering Technical Conferences and Computers and Information in Engineering Conference, 26th Conference on Mechanical Vibration and Noise [32].

References

[1] Moore, D. S., 2004, "Instrumentation for Trace Detection of High Explosives," Rev. Sci. Instrum., **75**(8), pp. 2499–2512.
[2] Moore, D. S., 2007, "Recent Advances in Trace Explosives Detection Instrumentation," Sens. Imaging Int. J., **8**(1), pp. 9–38.
[3] Kuznetsov, A. V., and Osetrov, O. I., 2006, "Detection of Improvised Explosives (IE) and Explosive Devices (IED)," *Detection and Disposal of Improvised Explosives*, Springer, Dordrecht, pp. 7–25.
[4] Östmark, H., Wallin, S., and Ang, H. G., 2012, "Vapor Pressure of Explosives: A Critical Review," Propellants, Explos., Pyrotech., **37**(1), pp. 12–23.
[5] Ratner, S. B., and Korobov, V. I., 1965, "Self-Heating of Plastics During Cyclic Deformation," Polym. Mech., **1**(3), pp. 63–68.
[6] Biot, M. A., 1958, "Linear Thermodynamics and the Mechanics of Solids," Third U.S. National Congress of Applied Mechanics, Providence, RI, June 11–14.
[7] Dimarogonas, A. D., and Syrimbeis, N. B., 1992, "Thermal Signatures of Vibrating Rectangular Plates," J. Sound Vib., **157**(3), pp. 467–476.
[8] Henneke, E. G., Reifsnider, K. L., and Stinchcomb, W. W., 1986, "Vibrothermography: Investigation, Development, and Application of a New Nondestructive Evaluation Technique," U.S. Army Research Office, Research Triangle Park, NC, Technical Report No. AD-A175 373.
[9] Renshaw, J., Chen, J. C., Holland, S. D., and Bruce, T. R., 2011, "The Sources of Heat Generation in Vibrothermography," NDT&E Int., **44**(8), pp. 736–739.
[10] Ratner, S. B., Korobov, V. I., and Agamalyan, S. G., 1972, "Mechanical and Thermal Fracture of Plastics Under Cyclic Strains," Sov. Mater. Sci.: A Transl. Fiz.-Khim. Mekh. Mater./Acad. Sci. Ukr. SSR, **5**(1), pp. 66–70.
[11] Katunin, A., and Fidali, M., 2012, "Self-Heating of Polymeric Laminated Composite Plates Under the Resonant Vibrations: Theoretical and Experimental Study," Polym. Compos., **33**(1), pp. 138–146.
[12] Paripovic, J., and Davies, P., 2013, "Identification of the Dynamic Behavior of Surrogate Explosive Materials," ASME Paper No. 2013-12755.
[13] Miller, J. K., and Rhoads, J. F., 2013, "Thermal and Mechanical Response of Particulate Composite Plates Under Direct Excitation," ASME Paper No. 2013-12138.
[14] Loginov, N. P., Muratov, S. M., and Nazarov, N. K., 1976, "Initiation of Explosion and Kinetics of Explosive Decomposition Under Vibration," Combust., Explos. Shock Waves, **12**(3), pp. 367–370.
[15] Loginov, N. P., 1997, "Structural and Physicochemical Changes in RDX Under Vibration," Combust., Explos. Shock Waves, **33**(5), pp. 598–604.
[16] Senchenkov, I. K., and Karnaukhov, V. G., 2001, "Thermomechanical Behavior of Nonlinearly Viscoelastic Materials Under Harmonic Loading," Int. Appl. Mech., **37**(11), pp. 1400–1432.
[17] Dinzart, F., Molinari, A., and Herbach, R., 2008, "Thermomechanical Response of a Viscoelastic Beam Under Cyclic Bending; Self-Heating and Thermal Failure," Arch. Mech., **60**(1), pp. 59–85.
[18] Rao, S. S., 2007, *Vibration of Continuous Systems*, Wiley, Hoboken, NJ.
[19] Jones, D. G., 2001, *Handbook of Viscoelastic Vibration Damping*, Wiley, Chichester, UK.
[20] Brinson, H. F., and Brinson, L. C., 2008, *Polymer Engineering Science and Viscoelasticity: An Introduction*, Springer, New York.
[21] Timoshenko, S. P., and Goodier, J. N., 1951, *Theory of Elasticity*, McGraw-Hill, New York.
[22] Incropera, F. P., DeWitt, D. P., Bergman, T. L., and Lavine, A. S., 2007, *Introduction to Heat Transfer*, Wiley, Hoboken, NJ.
[23] Paripovic, J., 2013, personal communication.
[24] Paz, M., 1997, *Structural Dynamics: Theory and Computation*, Springer, New York.
[25] Gustafsson, S. E., 1991, "Transient Plane Source Techniques for Thermal Conductivity and Thermal Diffusivity Measurements of Solid Materials," Rev. Sci. Instrum., **62**(3), pp. 797–804.
[26] Rich, B. R., 1953, "An Investigation of Heat Transfer From an Inclined Flat Plate in Free Convection," Trans. ASME, **75**, pp. 489–499.
[27] Vliet, G. C., 1969, "Natural Convection Local Heat Transfer on Constant-Heat-Flux Inclined Surfaces," ASME J. Heat Transfer, **91**(4), pp. 511–516.
[28] Goldstein, R. J., Sparrow, E. M., and Jones, D. C., 1973, "Natural Convection Mass Transfer Adjacent to Horizontal Plates," Int. J. Heat Mass Transfer, **16**(5), pp. 1025–1035.
[29] Tarver, C. M., Chidester, S. K., and Nichols, A. L., 1996, "Critical Conditions for Impact- and Shock-Induced Hot Spots in Solid Explosives," J. Phys. Chem., **100**(14), pp. 5794–5799.
[30] Mattos, E. C., Moreira, E. D., Dutra, R. C. L., Diniz, M. F., Ribeiro, A. P., and Iha, K., 2004, "Determination of the HMX and RDX Content in Synthesized Energetic Material by HPLC, FT-MIR, and FT-NIR Spectroscopies," Quím. Nova, **27**(4), pp. 540–544.
[31] Mares, J. O., Miller, J. K., Sharp, N. D., Moore, D. S., Adams, D. E., Groven, L. J., Rhoads, J. F., and Son, S. F., 2013, "Thermal and Mechanical Response of PBX 9501 Under Contact Excitation," J. Appl. Phys., **113**(8), p. 084904.
[32] Woods, D. C., Miller, J. K., and Rhoads, J. F., 2014, "On the Thermomechanical Response of HTPB Composite Beams Under Near-Resonant Base Excitation," ASME Paper No. 2014-34516.